

12. The universal slow RI-beam facility (SLOWRI)

(abstract)

Using modern atomic spectroscopy techniques extremely high precision measurements have become possible of various fundamental quantities of atomic nuclei. For instance, atomic masses and the hyperfine structure of ground state ions have been measured with a precision of $\sim 10^{-10}$ using ion trapping and laser spectroscopy techniques. Such techniques should play important roles also in studies of radioactive nuclear ions (RI). So far low energy RI beams have been provided mainly by ISOL (Isotope Separator On-line) facilities. However the available nuclides at ISOL facilities are limited, since chemical processes in production targets and in ion-sources are element dependent. The **slow RI-beam facility** (SLOWRI) at RIKEN aims to provide universal slow or trapped RI of high purity by combining a projectile fragment separator BigRIPS and a deceleration and cooling device, RF ion-guide [1]. This will allow a unique opportunity to perform precision atomic spectroscopy for a wide variety of RI, not available in so far existing facilities.

I. LIST OF COLLABORATORS

Spokesperson:

M. Wada* (*Atomic Physics Lab., RIKEN*)

Collaborators:

Y. Yamazaki, T. Kambara, Y. Kanai, T.M. Kojima, Y. Nakai, Y. Ishida, N. Ohshima, (*Atomic Physics Lab., RIKEN*), T. Kubo (*Cyclotrons Lab., RIKEN*), A. Yoshida (*Heavy Ion Physics Lab., RIKEN*), I. Katayama, T. Nakamura (*IPNS, KEK*), K. Okada (*Sophia Univ.*), H. Iimura (*JAEA*), H. Wollnik (*Giessen Univ.*), H. A. Schuessler (*Texas A&M Univ.*), V. Varentsov (*Radium Institute, St. Petersburg*)

II. FACILITY

The schematic overview of the SLOWRI facility is shown in Fig. 1. High energy RI-beams from BigRIPS are first decelerated by passing through a degrader. The energy distribution of the beams behind the degrader is as wide as 5A MeV. The beams are then injected into a catcher gas cell filled with helium buffer gas of ≈ 100 Torr. Because of the high ionization potential of He most radioactive ions end up as singly charged ions that can be manipulated by applied electric fields. A combination of electric dc fields and inhomogeneous rf electric fields in the gas drive the ions to a small exit nozzle (RF ion guide). There the ions are extracted from the gas cell and entered into a rf six-pole beam guide (SPIG)[2] that separates the ions from the He gas, forms a low-energy cooled beam and delivers this beam to high vacuum. This ion beam is electrostatically accelerated to ≈ 20 keV and mass separated by an ISOL to provide pure isotopic beams for experiments.

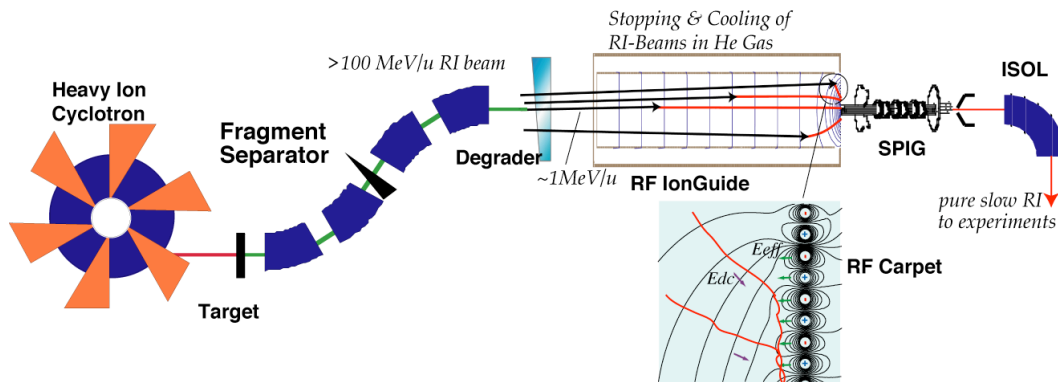


Fig. 1. Schematic overview of SLOWRI facility

1. Layout of the facility

The location and layout of SLOWRI as planned so far is shown in Fig. 2. High energy RI-beams from BigRIPS are provided through the D5 magnet of BigRIPS followed by a 6 degree deflector and a superconducting Q triplet. The energy degrader and the gas cell are located in the experimental room with a proper shielding. The 20 keV RI-beams are vertically deflected by mass separator magnets and then brought to the B3 floor with a low energy beam transport (LEBT). Various experiments can be performed at the B3 experimental room without background due to the production and deceleration processes. The B2 experimental room will be used for tall devices such as an EBIT (electron beam ion trap). The B1 floor is also reserved for future experiments, such as post acceleration.

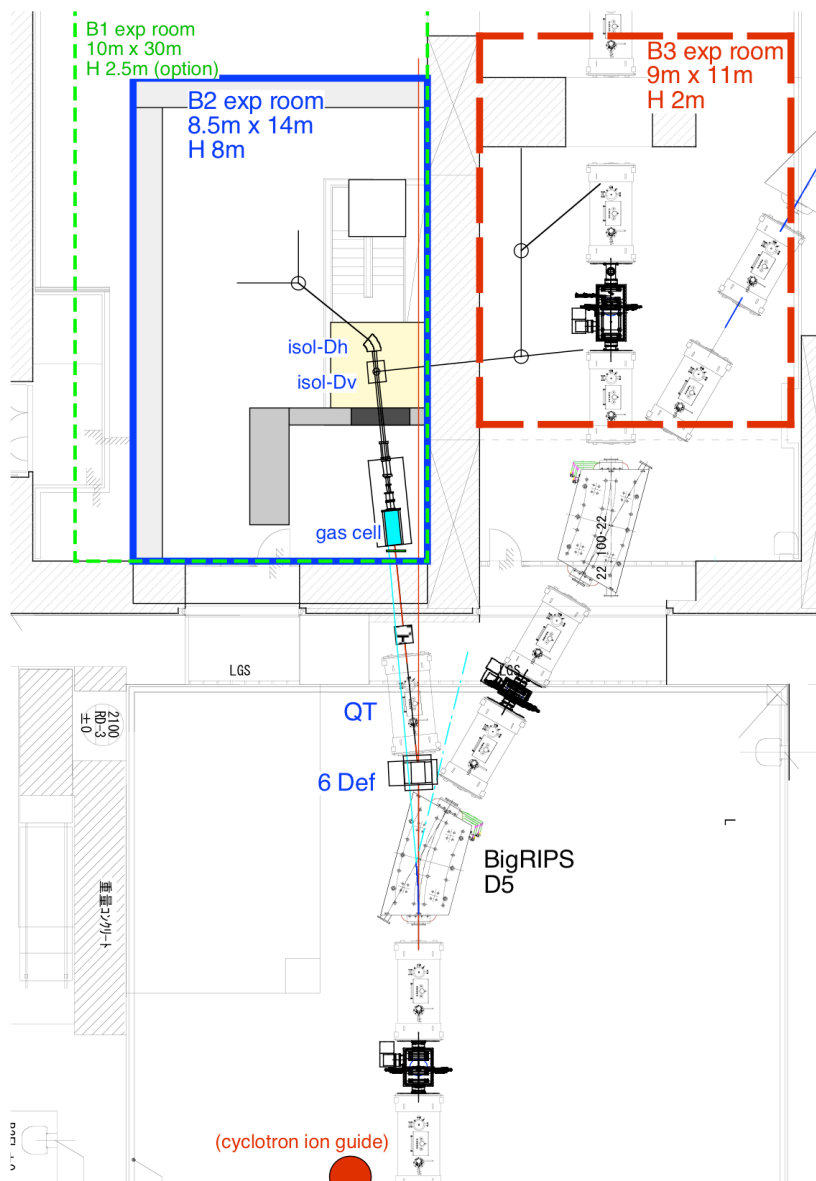


Fig. 2. Location of SLOWRI at RIBF.

2. High-energy beam line

The calculated ion optics for the high-energy, 9 Tesla meter, beam - including BigRIPS itself - is shown in Fig. 3. The initial beam emittance at the production target is assumed to be $(+0.5 \text{ mm}) * (+40 \text{ mrad})$ for the horizontal and $(+0.5 \text{ mm}) * (+50 \text{ mrad})$ for the vertical plane. At the energy degrader, a momentum dispersion of $38 \text{ mm}/\%$ is expected with a magnification of -2.1 . Since the focal point behind D4 already has large momentum dispersion, the transmission at the additional quadrupole triplet is not unity with the given dimension of the standard magnet. A 90% transmission can be obtained, however, by modifying the strength of four quadrupole triplets at the downstream of D3. In this case – unfortunately – no focal conditions are satisfied at the beam diagnostics chambers between D3, D4 and D5.

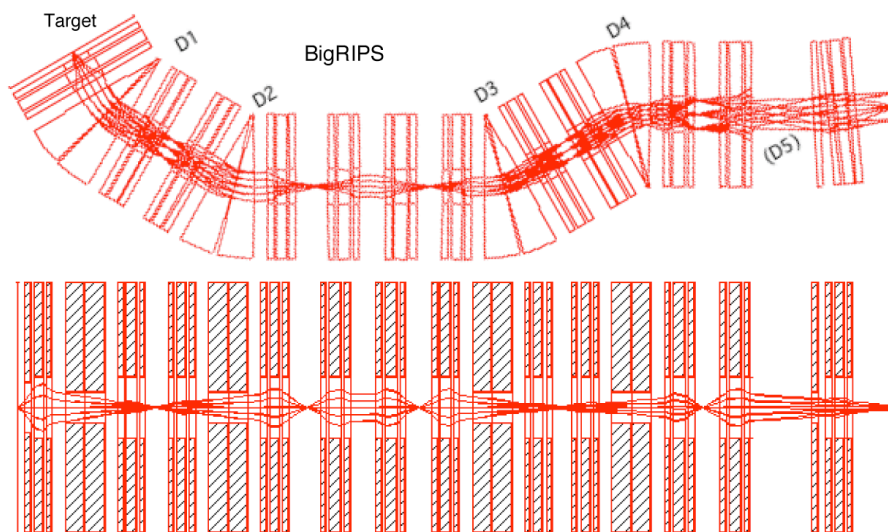


Fig. 3. Ion optical design for a high-energy beam branched off from BigRIPS. Horizontal (top) and vertical (bottom) views of the beam envelopes.

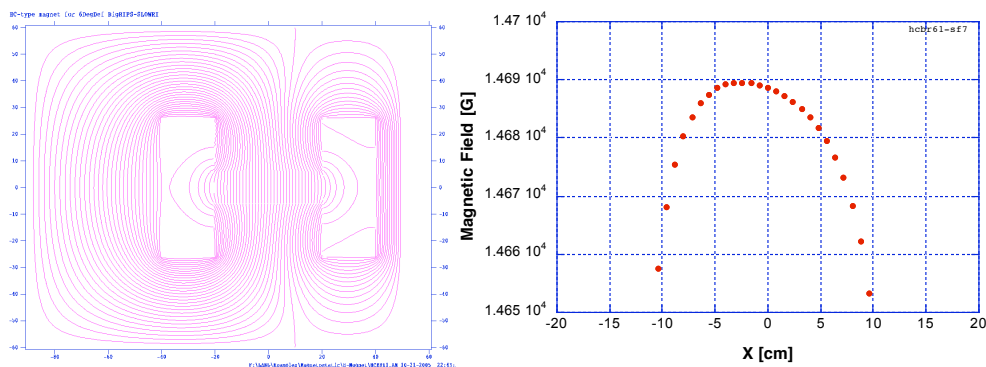


Fig. 4. Design of the 6-degree deflector as an asymmetric H-type magnet.

In this design the 6-degree deflector magnet is placed in a rather tight space to avoid interference to other magnets in the main-stream line. An asymmetric H-type magnet with additional saddle-shaped coils is planned to be build for this purpose. A typical design of the deflector magnet is shown in Fig. 4. A sufficient homogeneity of 0.2% for a beam-width of 20 cm with a 40-cm pole width and a 12-cm pole gap is expected.

3. Ion guide gas cell

As long as relatively heavy ($A > 20$) ions are the main beams to be supplied at SLOWRI, the length of the gas cell can be reduced to 1 m. The stopping efficiency of the cell filled with 100 Torr He gas combined with the mono-energetic degrader at the momentum dispersive focal plane for $A=100$ ions of 350A MeV is larger than 90% (Fig. 5).

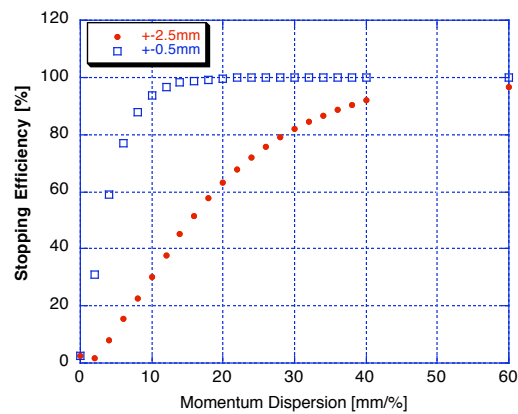


Fig. 5. The stopping efficiency in a 1-m-long gas cell with 100 Torr He gas for $A=100$, 300A MeV RI-beams from BigRIPS having a momentum spread of $\pm 3\%$. Boxes indicate beam spot sizes as caused by initial beam emittances of $(+0.5 \text{ mm}) * (\pm 40 \text{ mrad})$ while red dots indicate for 5 times larger beam spot sizes considering emittance blowup effects in the target and the degraders of BigRIPS.

The gas cell contains a cylindrical rf-carpet and a planar rf-carpet in the central cylinder (Fig. 6). This central cylinder is thermally isolated from the outer cylinder and attached to a cryogenic head or a refrigerator tube in order to reduce impurities in the gas. The cylindrical rf-carpet transports thermalized ions to the downstream-end of the cell by dc fields parallel to the cylinder axis. The planar rf-carpet transports the ions arriving from the entire cell to the exit nozzle at the center. The key function of the rf-carpets is an *ion-barrier* [3] to keep ions reaching the surface of the electrodes. The barrier field is realized by rf-gradient fields produced by the many concentric ring-electrodes of the rf-carpet. A typical distance between neighboring ring-electrodes is only 0.28 mm. Rf voltages of

≈ 150 V with a frequency of ≈ 10 MHz are applied between the *odd*- and the *even*-numbered rings of the carpet [1]. A typical ion trajectory at the planar rf-carpet is shown in Fig. 8. There is also a new cylindrical rf-carpet which reduces the efficiency limitations due to space-charge forces caused by He^+ ions produced during the stopping process of the incoming beam. This space-charge namely forces many thermal ions to move to the cylindrical wall instead of going to the planer rf-carpet due to a potential *ridge* appeared at the central axis of the cell [4]. Barrier fields of < 5 V/cm (Fig. 7) at this cylindrical rf-carpet already keep such ions from sticking to the wall and transport them to the planar rf-carpet.

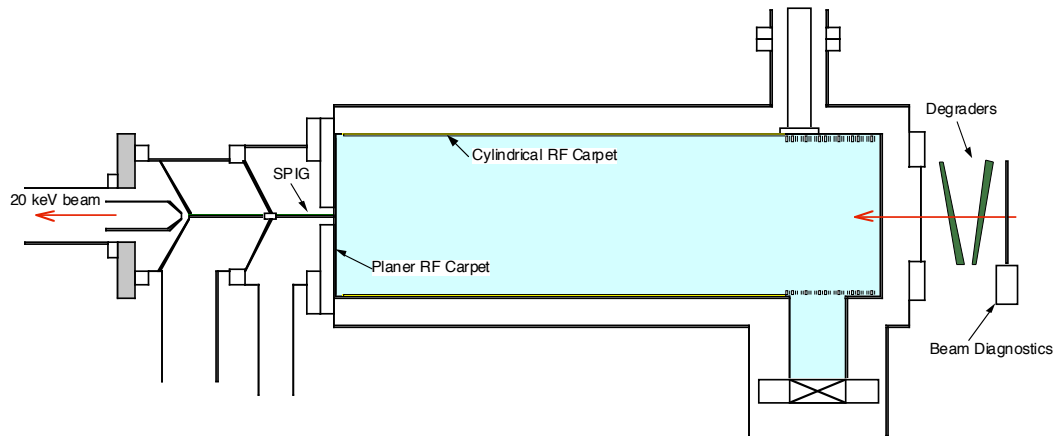


Fig. 6. Schematic of the new ion guide gas cell.

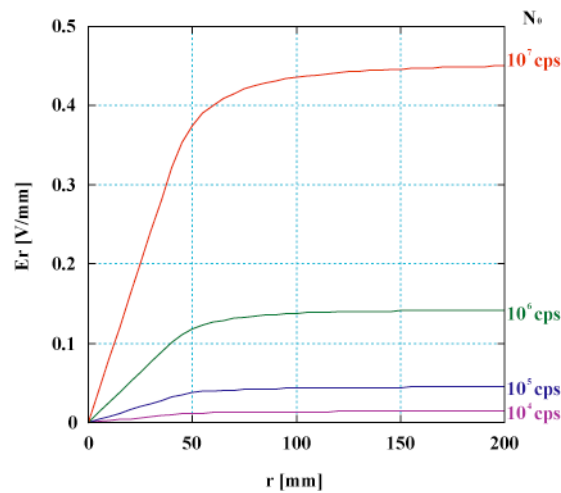


Fig. 7. Radial electric field due to space-charge caused by the incoming beam intensities of 10^{4-7} counts per second [4].

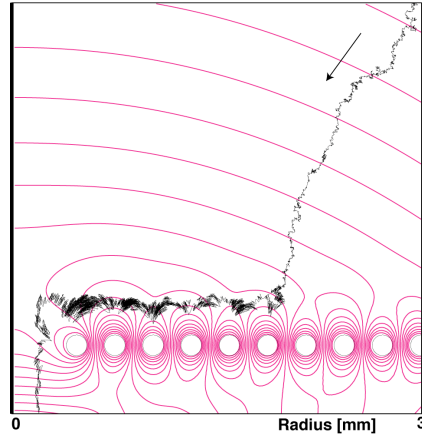


Fig. 8. Ion trajectory at the nozzle part of planar rf-carpet [4].

The ions that are extracted from the exit nozzle of the planar rf-carpet are guided by SPIG (a rf sextupole ion beam guide) [2] to a high vacuum vessel through two differential pumping sections. The SPIG separates ions from the residual buffer gas but also provides cooling and bunching capabilities [5]. In the present design, however, impurity ions originating from impurity molecules in the gas still dominate the ion beam. Since they quickly fill the small potential well of the SPIG-trap, bunching capabilities will be implemented further downstream behind the mass separator.

4. Mass separator

The cooled slow ions from the gas cell are accelerated by an electrostatic voltage of up to 30 kV and brought to a mass separator in order to separate from impurity ions. The radioactive nuclear ions from BigRIPS are all from the same isobar, but can contain different isotones. A mass separator that features a mass resolving power of ≈ 1000 should be capable of removing all undesired isotones and stable impurities. The planned ion optical design of the mass separator is shown in Fig. 9 together with a part of LEBT (low energy beam transport).

In the present design, a mass resolving power of 700 for the initial emittance of $(+0.5 \text{ mm}) * (+- 20 \text{ mrad})$ is achieved. The cooling capability at SPIG, however, should provide smaller emittance than the design value.

Mass analysis is performed by two 45 degree dipole magnets ($r=500 \text{ mm}$) after phase-space matching which is achieved by four electrostatic quadrupoles. Second- and third-order aperture aberrations are widely compensated by an octopole element and curved boundaries of the sector fields. Mass analyzed ions are then guided by achromatic deflector fields to the B3 floor.

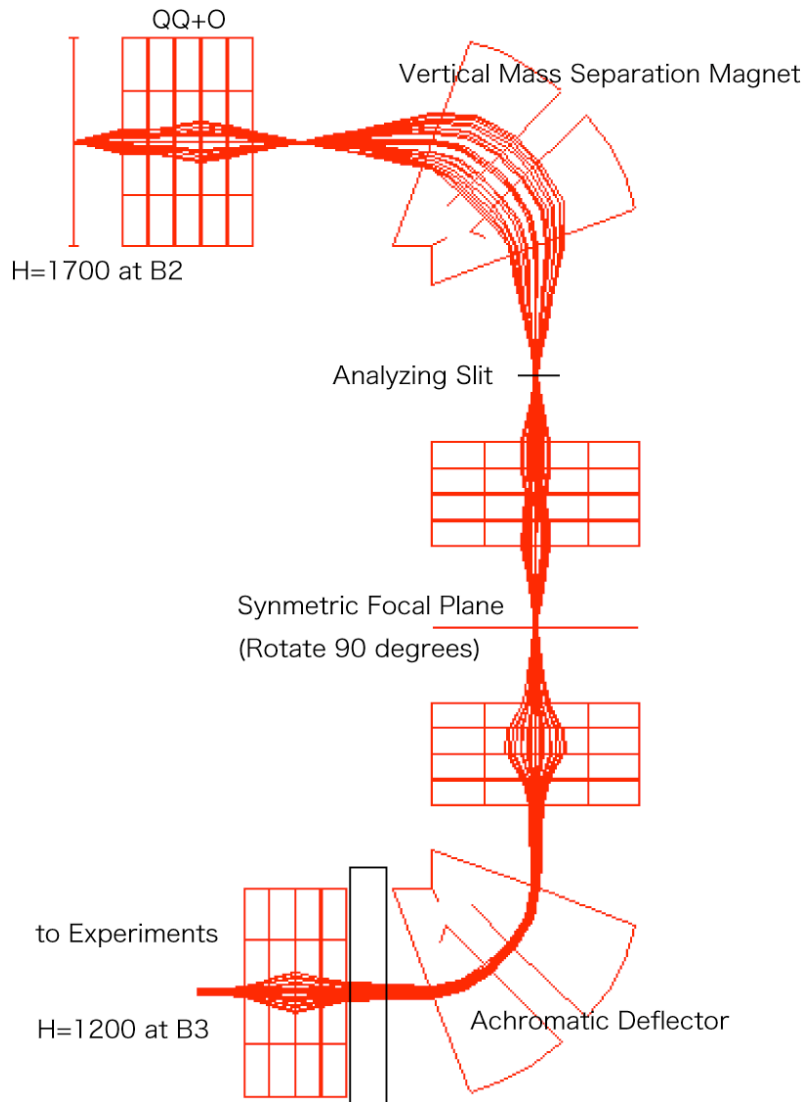


Fig. 9. Ion optical design of the planned mass separator and the LEBT to the B3 floor.

5. Low energy beam transport and B3 experimental room

Mass-separated 30-keV pure-ion beams are supplied to various experimental setups in the B3 experimental room through a LEBT. The beam transport lines to the other experimental room are future options for the moment. The planned layout of the B3 experimental room is shown in Fig. 10. Some experiments require stopped ions at the ground potential experimental setup. For this purpose, the entire beam transport line including the mass separator can be located at a high voltage potential while the gas cell, the buncher and the experimental setup can be placed at the ground in this particular configuration.

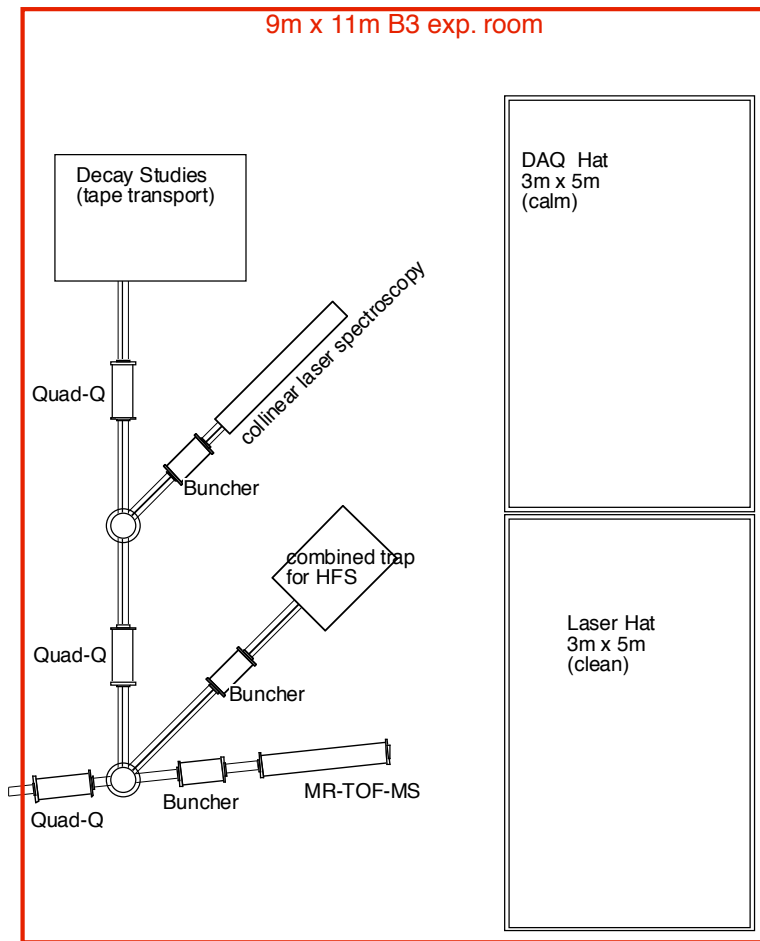


Fig. 10. Planned experiment layout in the B3 experimental room and beam delivering lines.

6. Beam buncher

Beam bunching and cooling of ISOL beams has been an important concern for IGISOL systems especially when the beam is used for laser spectroscopy. The beam emittance and the energy-spread of an IGISOL are quite large compared to those of a conventional ISOL. A beam bunching and cooling device using an RFQ and buffer gas cooling for IGISOL was developed at Jyvaskilla [6]. Similar devices with new improvements are planned to be used in front of the experimental setups which require bunched beams. The additional functions are: 1) the use of a high order rf multipole instead of a quadrupole, 2) the use of cryogenic head to cool the trap electrodes and the buffer gas, and 3) the use of multi-stacking method by gating the entrance potential synchronized to the prebuncher pulse, which will be placed a few meter upstream of the buncher trap. These new functions will provide higher bunching efficiencies and cooler ion bunches.

III. STATUS OF R&D

Since the group has proposed the idea in 1997 it has worked on the development of the rf ion guide system to decelerate energetic radioactive nuclear ions, to cool them and to accumulate them in an ion trap. The system obtained a high overall efficiency of $\approx 5\%$ for 100A-MeV Li-8 ions from the present RIKEN fragment separator RIPS. Recently radioactive Be isotope ions were trapped in an on-line trap and precision laser spectroscopy was performed for the first time.

1. The prototype rf ion guide system

Development of the prototype rf ion guide setup has been carried out at the E6 vault of the present RIKEN accelerator facility where $\approx 100A$ MeV RI-beams are available with various intensities. The gas cell is located not at the ordinary experimental port (F3), but at the second focal point (F1') of the first dipole magnet passing through the not-excited second dipole magnet. The new location has the advantage that the momentum dispersion at the focal plane is as large as $35\text{mm}/\%$ which allows us to use a wedge-shaped energy degrader as a “nono-energetic degrader”. A more practical advantage is that there are less conflicts with other experiments. A drawback is that the intensity of impurities in the beams is often much higher than the ions of interest.

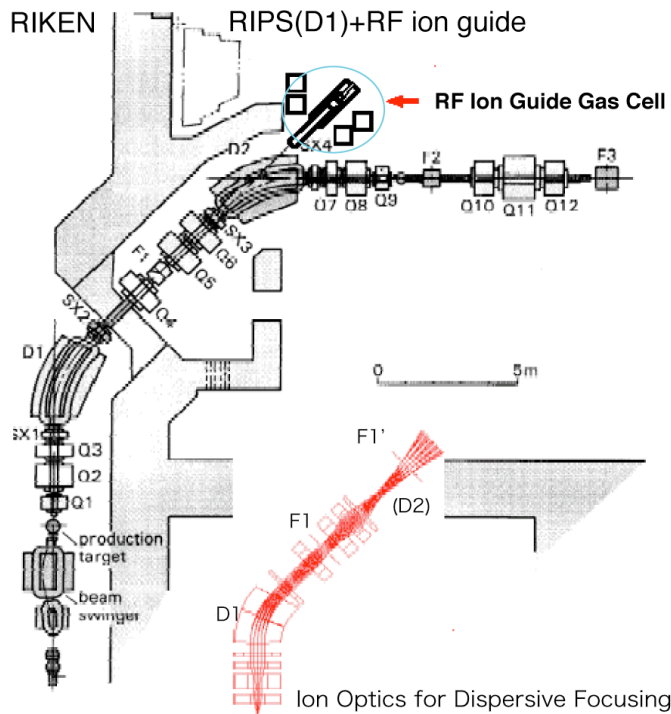


Fig. 11. RIKEN fragment separator RIPS and prototype rf ion guide

Since the energy distribution behind the degrader (Fig. 12) is very large in case of light mass nuclei such as Li the stopping efficiency in the gas cell is miserably small if a flat plate degrader is used, or the momentum dispersion at the degrader is small. The combination of a highly momentum dispersed beam and a wedge-shaped degrader provided gains of more than one order of magnitude for the stopping efficiency.

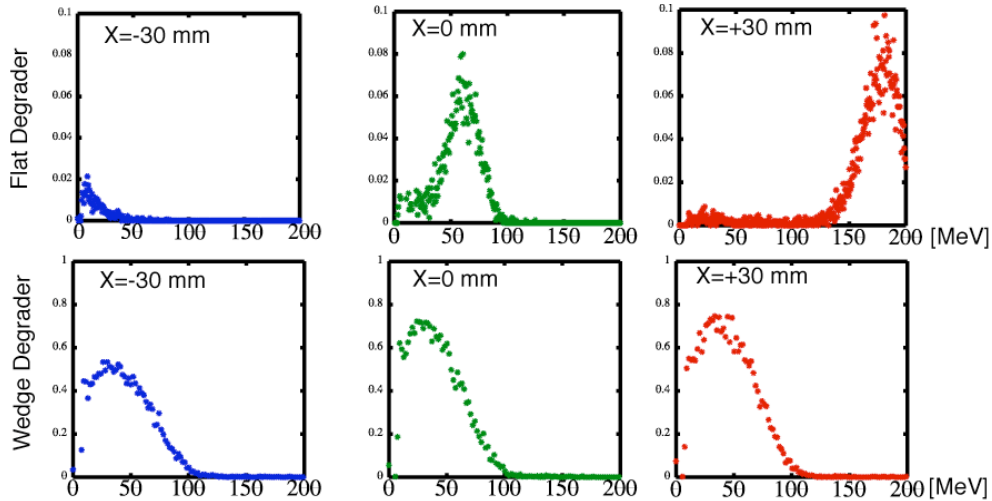


Fig. 12. The energy distributions of Li-8 ions behind the energy degrader of flat plate (top) and of wedge shape (bottom) as function of the horizontal position from the beam center.

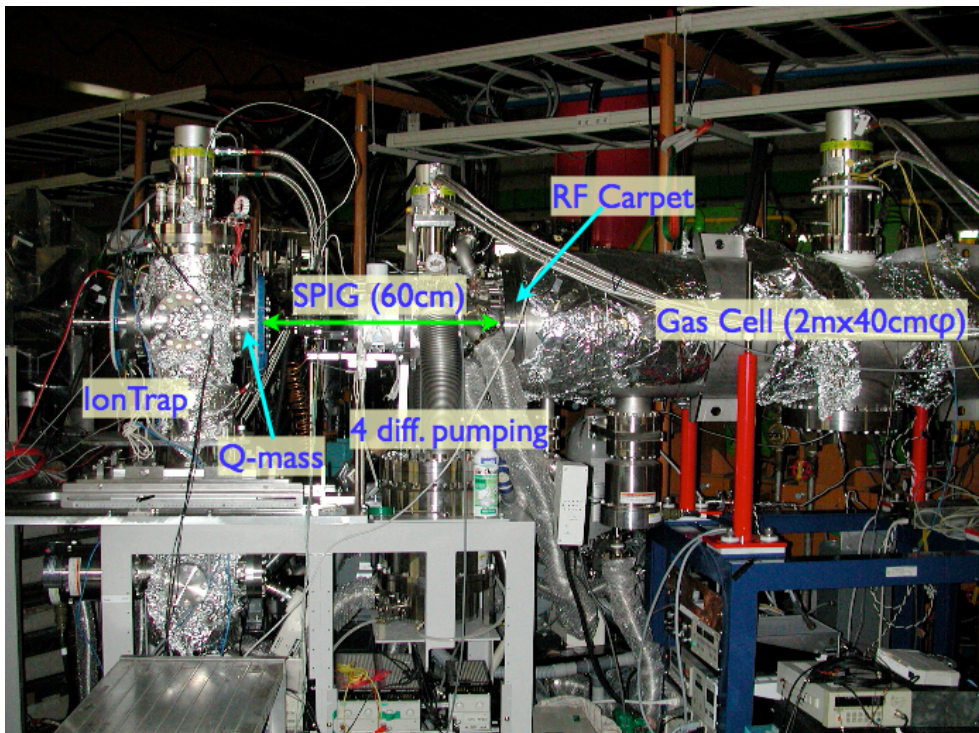


Fig. 13. Gas cell and beam line to spectroscopy trap.

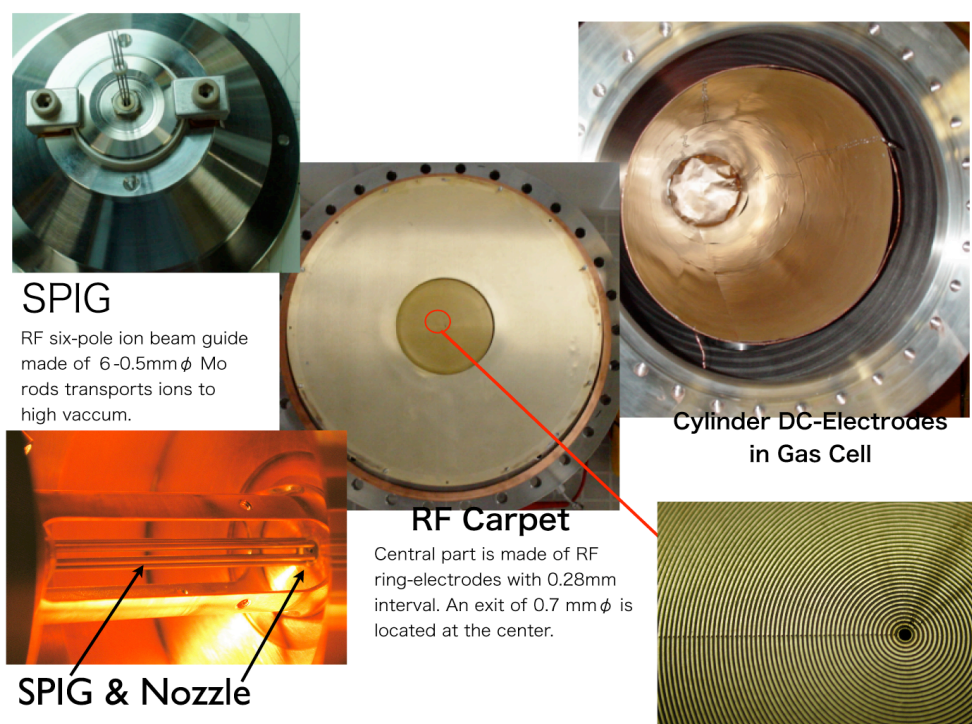


Fig. 14. Photos of the parts of rf ion guide

An overview of the existing experimental setup including the “spectroscopy trap” is shown in Fig. 13. The used gas cell is 2 m long and has a diameter of 40 cm. There is a cylindrical tube in which dc electrodes produce an axial dc field and a rf-carpet electrode at the downstream end of the cell (Fig. 14). The dc field in the cylinder guides the ions to the rf-carpet. The rf-carpet is made of a printed circuit board featuring many concentric ring-electrodes are presented. Rf voltages of ≈ 150 V with a frequency of ≈ 13 MHz are applied between neighboring rings to produce a rf gradient field. The strength of the barrier force due to the rf gradient field is proportional to the mass of ions, the square of the applied rf voltage and the reciprocal of the pressure of the gas. For light ions, the pressure cannot be too high. In the present conditions, 100 Torr is an appropriate pressure of the gas at which the stopping efficiency of the 2-m-long cell is as small as 11% for ≈ 100 A MeV Li-8 ions from RIPS.

In the yield test experiments for Li-8, the intensity of slow Li-8 ions was measured by the number of delayed-alpha particles detected in a silicon detector located behind the nozzle of the rf-carpet or behind a short (120 mm) SPIG. The overall efficiency here is defined as the ratio of the detected number of alpha particles to the number of total incoming ions of Li-8 from RIPS while the ion guide efficiency is the ratio of the number of alpha particles to the number of Li-8 ions stopped in the cell.

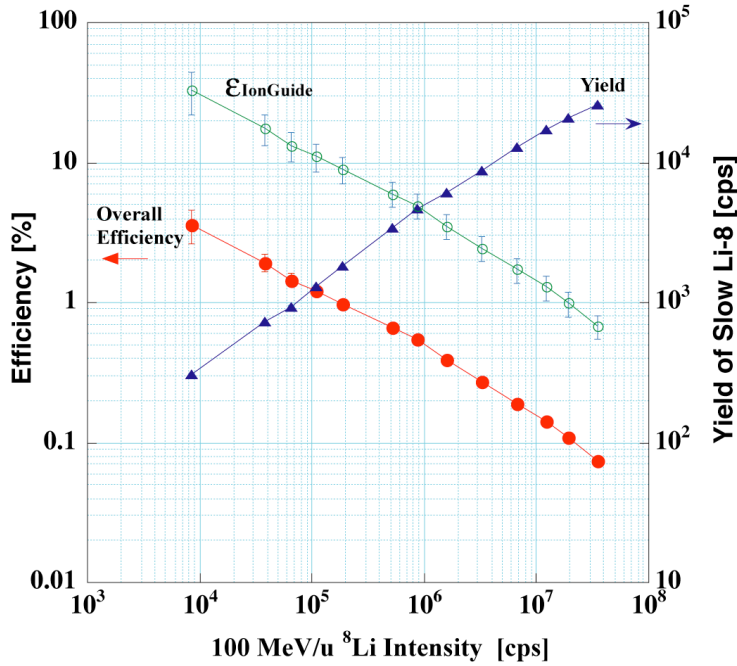


Fig. 15. The efficiencies and the yield of low-energy Li-8 ions.

A typical result is shown in Fig. 15. The efficiencies decrease when the intensity of the incoming beam increases. The dependence is almost inversely proportional to the square-root of the beam intensity. This phenomenon is successfully explained in the recent paper [4] as briefly described in the next section.

2. Space charge effect in the catcher gas cell

When incoming energetic ions stop in He gas, one He⁺ ion-electron pairs is produced for every 40 eV of energy loss of the primary ion. Since the mobility of electrons in the gas is three orders of magnitude faster than that of ions, therefore, electrons can be quickly leave the gas due to the applied external electric fields while He⁺ ions slowly drift along with the electric force lines. For high-intensity beams, many He⁺ ions are presented at the central part of the cell thus causing strong radial space-charge fields in the cell. The production rate of He⁺ ions is proportional to the intensity of incoming beam, though the He⁺ ions drift themselves due to the electric fields caused by a space-charge whose density is proportional to the square-root of the incoming beam intensity at equilibrium. The space-charge distribution in the gas cell was analytically solved [4] from which the existing electric fields (see Fig. 16) were calculated by the POISSON code. The ion trajectories in these fields are also shown in this figure. At higher intensities, only those ions stopped close to the rf-carpets can be extracted while all other ions move towards the cylinder wall.

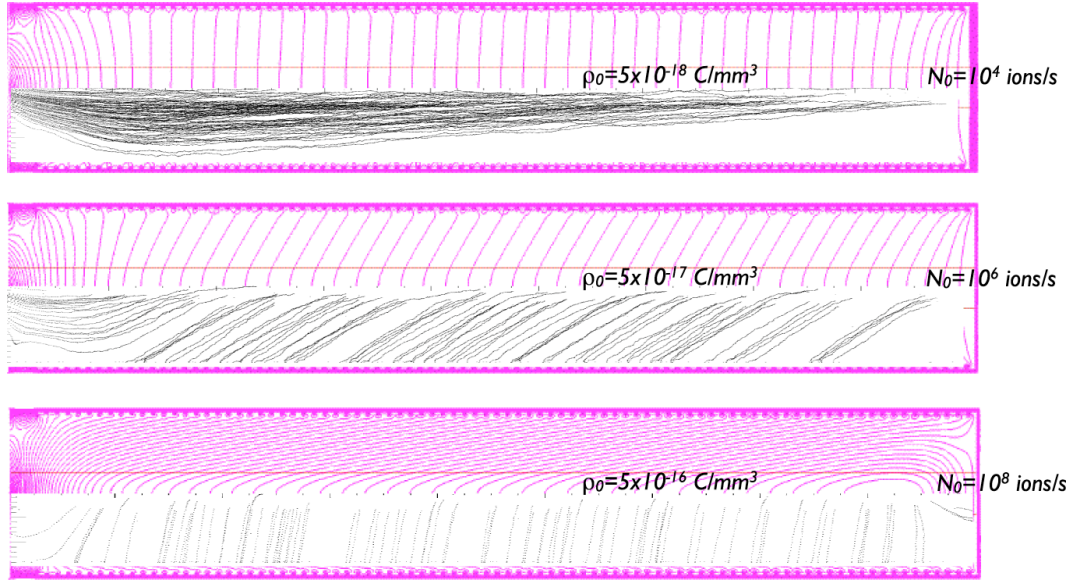


Fig. 16. DC electric fields in the gas cell distorted by space-charge are shown in the top halves and ion trajectories in the cell in the bottom halves at different intensities of the incoming primary beam.

Though the dependence of the efficiency is not only on the space-charge density but also on the geometry of the system, the efficiency is approximately inversely proportional to the space-charge density. In total thus, the efficiency is inversely proportional to the square-root of the incoming beam intensity. This is a qualitative explanation of the experimental results while a quantitative explanation is given in ref. [4].

3. Spectroscopy of radioactive Be isotopes

As a first application of the prototype rf ion guide setup, we have worked on laser spectroscopy of trapped Be isotopes aiming at the study of the neutron halo through the Bohr-Weisskopf effect [7]. A linear Paul trap has been used for this experiment to which slow Be^+ ions are brought through a 500-mm-long SPIG through four differential pumping sections. The assembly of the trap electrodes is attached to a cryogenic pump-head to keep an ultra-high vacuum even when a buffer gas is introduced.

Be-10, a very long-lived isotope, was chosen to be the first radioactive isotope to be investigated in the on-line spectroscopy trap. Since there was a problem in the long SPIG, the buffer gas pressure was adjusted to only 10 Torr which resulted in only 10 atoms per second of slow Be-10 ions. Impurity ions from the cell were rejected by a rf quadrupole mass filter placed in front of the spectroscopy trap. Since the bunching function at the SPIG is not effective at such low-pressure gas-cell conditions, a continuous ion beam was directly introduced to the spectroscopy trap where a He buffer gas of up to 10^{-3} Torr existed

during the accumulation period. This buffer gas was quickly removed when the accumulation period was terminated. A cw laser radiation at 313 nm was then introduced to the trap when we observed fluorescence from the trapped ions. Fig. 17 shows the obtained fluorescence spectrum of laser cooled Be-10 ions. The number of trapped ions was approximately 100 and the temperature of the ions was measured to be 0.8 K from the Voigt profile of the spectrum. The resonance frequency was evaluated to be 957,414.825(10)(586) GHz. The first uncertainty is due to the statistical error and the second is due to the calibration inaccuracy. The present value is consistent within the error with the theoretical values calculated by Yamanaka [8]. This confirmation is very useful when we search for the other Be isotopes. Hyperfine structure spectroscopy of Be-7 and Be-11 will be performed soon.

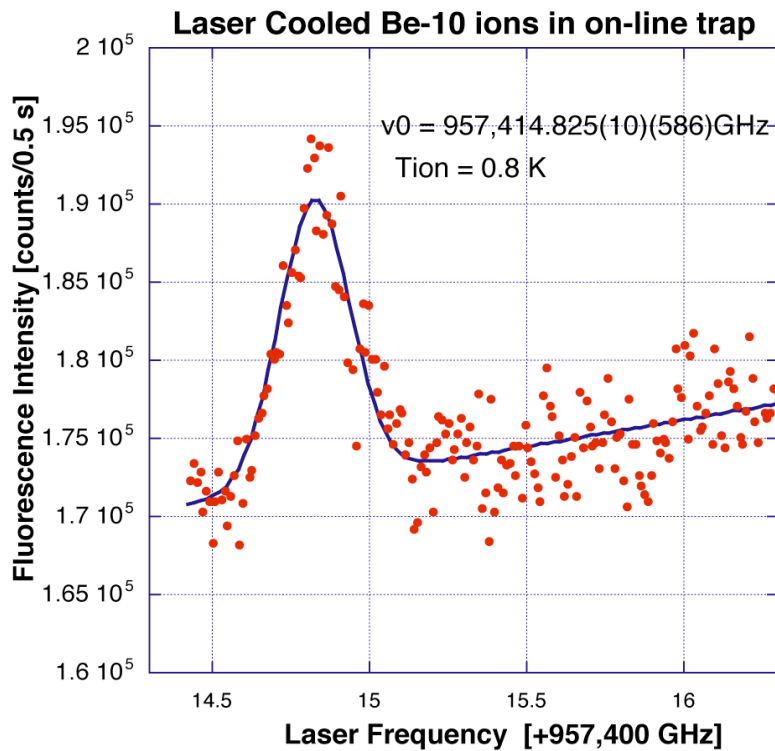


Fig. 17. The laser induced fluorescence intensity of laser cooled Be-10 ions in an on-line ion trap plotted as function of the laser frequency.

4. Possible improvements for the future facility

There are several possible solutions to overcome the present problems found in the prototype system and to improve its performance. Some of these possibilities we plan to test at RIKEN. The goal of these developments is to achieve *high efficiency* even for high intensity beams, to have a *fast extraction* capability in order to obtain very short-lived nuclei, and to have *high-purity* beams for nuclei of *all elements*.

Full cover carpet

A straight forward solution to overcome the space-charge problems is to cover large part of the surface of the cell with an rf-carpet. In this way, the effective volume can be increased even for high intensity beams. This possibility is already included in the new gas cell for SLOWRI, however, it is practically impossible to be used for very light ions. The light ions require very high rf frequency voltages which to supply to wide area of rf-carpet is difficult. In the new gas cell, also provisions are made to keep the temperature of the cell low in order to reduce the density of impurity atoms and molecules.

Fair-wind gas cell

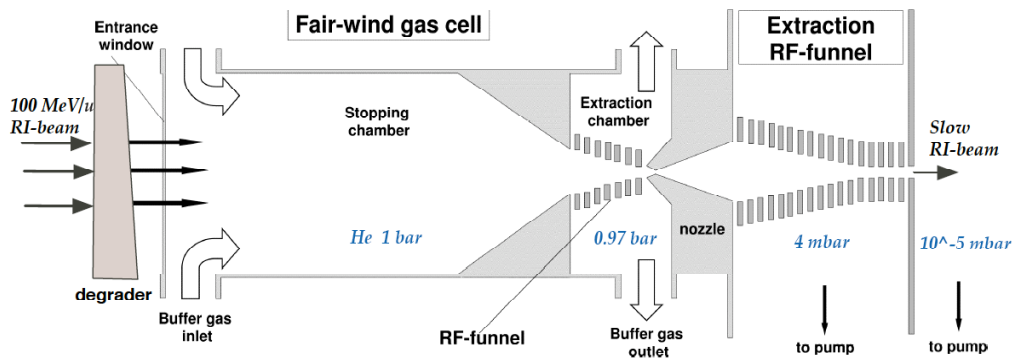


Fig. 18. Schematic of the fair-wind gas cell concept.

The *fair-wind* concept as initially proposed by Varentsov [9] aims to operate the gas cell at a pressure of 1 bar which allows high stopping efficiency even in a small gas cell. The transport of thermal ions here must be carried by the gas flow. This would be a *renaissance* of the original IGISOL concept, though the throughput of the gas flow is increased very much much by evacuating not only through the exit nozzle, but mainly through the gaps of a rf-funnel. The principle of such rf-funnel is the same as that of a rf-carpet. Thus, it is not simple to obtain a sufficiently strong barrier field in a high-pressure buffer gas. Numerical simulations [10] showed, however, that the strength of the static force due to the gas flow is much smaller than that of the dc electric field which is used in the ordinary rf-carpet to bring ions to the exit. The lack of dc electric fields at the rf electrodes of the rf-funnels of a fair-wind gas cell would simplify the rf circuit considerably.

Since there are no external dc electric fields in the cell, He^+ ions, electrons and radioactive ions move together with the gas flow as a weak plasma. Ion-electron recombination or chemical reactions in the plasma still must be investigated, however. Furthermore, when ions come close to the rf-funnel, the electrons are quickly removed from the plasma due to the rf fields which will cause strong space-charge forces due to remaining ions. Thus noticeable strength of the dc electric fields will be presented at the rf-funnel.

One possible method to separate the undesired He^+ ions in the fair-wind cell is the proposed “*head-wind* gas cell” which makes use of the fact that the mobility of He^+ ions in He gas is about half of the mobility of impurity atomic ions. If an appropriate dc electric field is applied against the gas flow, thus He^+ ions move with the gas flow while impurity atomic ions move with the electric field. This condition can be tested by additional dc electrodes in the cylindrical part of the fair-wind gas cell and an extra gas port at the middle of the cell. Such a gas cell is now under preparation.

Cyclotron ion guide

The concept of a *cyclotron ion guide* was first proposed by Katayama et al [11] in 1997. In fact, the present rf ion guide scheme originated in a part from this concept. In this scheme, energetic RI-ions are injected into a weakly focusing cyclotron magnet through a thin degrader. These ions then circulate in the magnetic field and losing the energy by ionizing buffer gas in the cell where a relatively low He gas pressure exists. When ions are stopped everywhere in the cell, a large portion of them is guided to an exit nozzle by the electric fields of rf-carpets without sticking to the wall of the cell.

Advantages of this scheme are: 1) the stopping path length for energetic ions can be very long, i.e., more than 100 m, which results in a high stopping efficiency even at lower pressure in the buffer gas. 2) The drift path length for thermal ions toward the exit nozzle is short and the velocity is fast due to the low gas pressure, which allows fast extraction of RI ions. The most important benefit in view of the present space-charges problem is that the region of high space-charge and the region of thermal ions’ drift motion are well separated. The main disadvantage is that an expensive large cyclotron magnet is necessary.

An old magnet used for designing the INS SF cyclotron has been reserved for a prototype setup for the cyclotron ion guide to be tested at RIKEN. Recently Bollen et al at MSU also investigated a similar scheme [12] and a collaboration of MSU and RIKEN has been started.

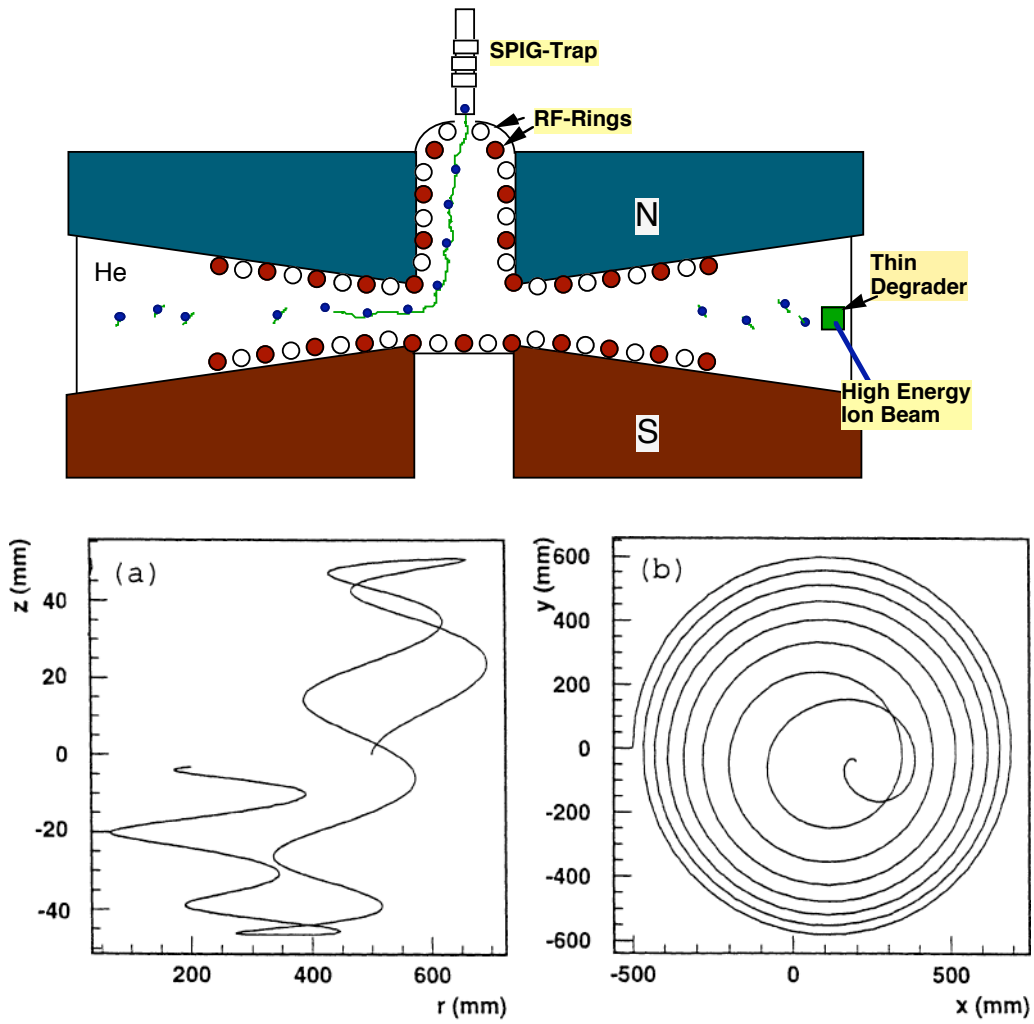


Figure 2. A trajectory of a 5 MeV/u $^{11}\text{Be}^{4+}$ ion coming out of a proper Ta energy degrader at $R = 50$ cm and 5000 Pa He gas. The ion starts with an azimuthal velocity of $v_x = 3.1 \times 10^7$ m/s and $v_z = 4.2 \times 10^5$ m/s at $(x_0, y_0, z) = (-500, 0, -3)$ mm. The charge state of ion is assumed to follow a charge equilibrium given in [8]. Magnetic field is taken to be $B_z = B_0(1 - 0.25r/R)$ and $B_r = 0.25B_0z/R$ with $B_0 = 17$ kG. The result shows (a) the ion orbit in (z, r) -plane, and (b) the ion orbit in (x, y) -plane.

Fig. 19. Schematics of the cyclotron ion guide setup (top) and an ion trajectory in the cyclotron ion guide gas cell [11] (bottom).

IV. SPECIFICATIONS OF THE FACILITY

Beam intensities at SLOWRI as expected in 2007 are shown in Fig. 20. These values are based on the evaluated beam intensities of energetic RI-beams at BigRIPS [13] and the present performance of the RF ion-guide. There are two limiting factors for the efficiency of SLOWRI. One is the lifetime of the nuclei of interest. For nuclei have half-lives >400 ms, the effective volume is assumed to be unity while for ions of shorter half-lives, the volume is proportional to the lifetime. The other is the space-charge effect. The effective volume decreases inversely proportional to square-root of the incoming beam intensity and the masses of nuclei. In total we expected that in the year 2007 more than 2800 nuclides will be available with intensities higher than 0.01 ions per second.

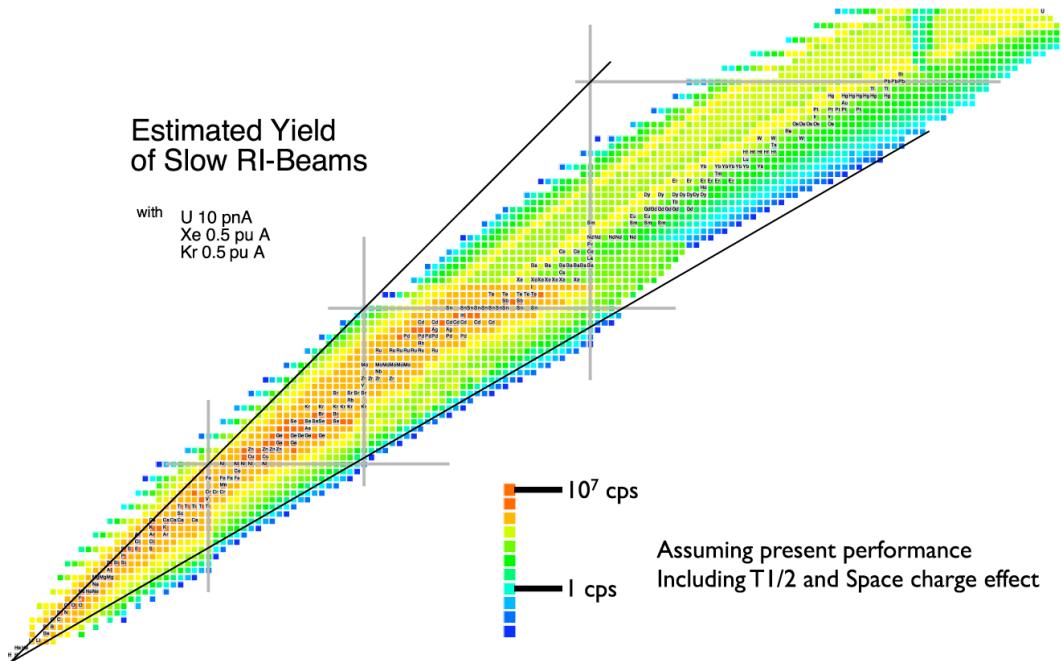


Fig. 20. Expected beam intensities of low-energy RI-beams at SLOWRI in the first years.

Characteristics of the SLOWRI facility are summarized to be:

1. A wide range of nuclides
2. High purity, no isobar or isotone contamination
3. Small emittance (1π mm mrad) and short bunched beams
4. Variable energy range, in traps (~ 0 eV) or accelerated (1~10 keV, 1 MeV/u)
5. Human accessibility during on-line experiments

In the isolated experimental room the slow RI-beams will be transported to various experiments.

The SLOWRI provides a wide variety of nuclides as pure and cooled low-energy beams and or stored ion clouds in ion-traps.

- Number of nuclides >2800 (for > 0.01 atom/s) (Fig. 20)
- Available elements all elements from BigRIPS
- Beam energy $\sim 0\text{eV}$ (trap), 1~50 keV, 1 MeV/u (option)
- Beam emittance $< 10 \pi$ mm mrad
- Beam intensity Shown in Fig. 20.

V. COSTS AND MANPOWER

SLOWRI is not a proposal of an experiment but a proposal of a new facility belongs to RIBF. A reasonably large investment in both budget and manpower should be made. Detail of the cost estimation is in progress.

Manpower request

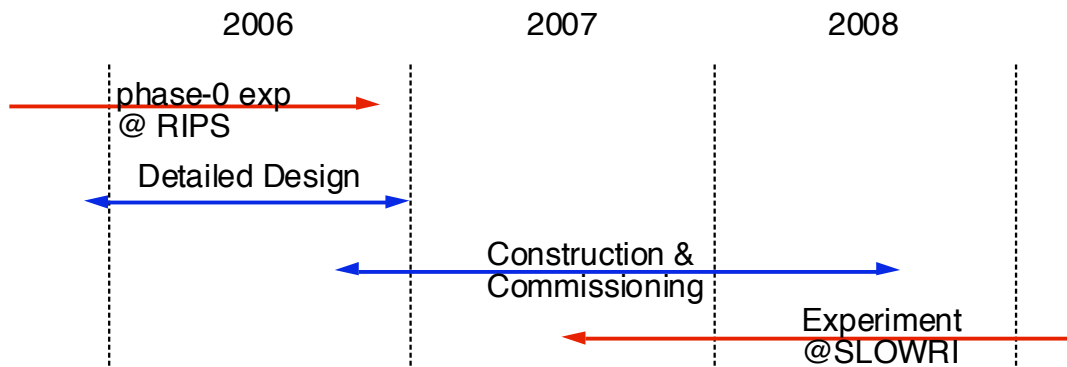
- Permanent Researcher 2
- Permanent Technical staff 2
(Mechanics, Electronics, Laser, Maintenance)
- Postdoctoral Fellow 3~5 (at least one for each experiment)

It should be noted that we organize several workshops and a researchers' association to invite or to collaborate with researchers outside RIKEN to perform their own experiments at SLOWRI.

Cost estimation (preliminary)

- High Energy Beam Transport (excl. SCQT) 20 M yen
- New gas cell and extraction setup 50 M yen
- ISOL and beam guidance 50 M yen
- Installation of experimental setups 50 M yen
- Miscellaneous (Infrastructure, Shielding etc) 30 M yen

Schedule



VI. PHYSICS SUBJECTS TO BE INVESTIGATED AND OBSERVABLES TO BE MEASURED

Various static properties of nuclei can be determined through precision atomic spectroscopy of trapped unstable ions and beams of low energy unstable nuclei. Typical quantities to be measured at SLOWRI are:

1. Atomic masses
2. Charge radii
3. Valence neutron radii
4. Nuclear moments
5. Abundances of protons and neutrons at the surface of nuclei

In addition, the obtained pure and small emittance beams of low energy unstable nuclei can be injected into other accelerators for further acceleration and into other experimental facilities. One such possibility of the latter could be the SCRIT facility, where electron scattering experiment could be performed to determine nuclear charge form factors. Conventional nuclear decay spectroscopy is also an important application at SLOWRI where various pure radioactive nuclei are provided in a low-background environment.

VII. MAJOR EXPERIMENTAL CASES

1. Mass measurements

The atomic mass is one of the most important quantity of a nucleus and has been studied in various methods since the early days of physics. Among many methods we chose a multi-reflection time-of-flight (MR-TOF) mass spectrometer (Fig. 21). Slow RI beams extracted from the RF ion-guide are bunch injected into the spectrometer with a repetition rate of ~ 500 Hz. The spectrometer consists of two electrostatic mirrors between which the ions travel back and forth repeatedly. These mirrors are designed such that energy-isochronicity in the flight time is guaranteed during the multiple reflections while the flight time varies with the masses of ions. A mass-resolving power of >60000 has been obtained with ~ 500 reflections in a 30 cm length spectrometer (Fig. 22) [14]. The mass-resolving power at present is more than 100,000 which should allow to determine ion masses with an accuracy of 10^{-7} . This accuracy is lower than that obtained in a Penning trap mass spectrometer, however, it is sufficient to study many r-process nuclides, for instance. The advantages of the MR-TOF spectrometer are: 1) short measurement periods, typically 2 ms, which allows all neutron rich nuclei to be investigated, 2) the device is compact and its operation is simple, especially, it is independent from the all upstream devices, accelerators and fragment separators, 3) ions of more than isobars can be measured simultaneously, so that mass reference can easily be established in the mass spectra. In total, the number of measurable nuclides within a limited beam time would be larger than that can be achieved by other methods. It should be noted here also that this method can be used even during a low-duty parasite beam time.

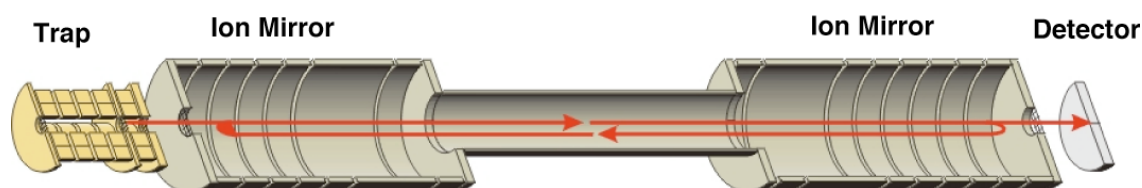


Fig. 21 Schematic of the multi-reflection time-of-flight mass spectrometer.

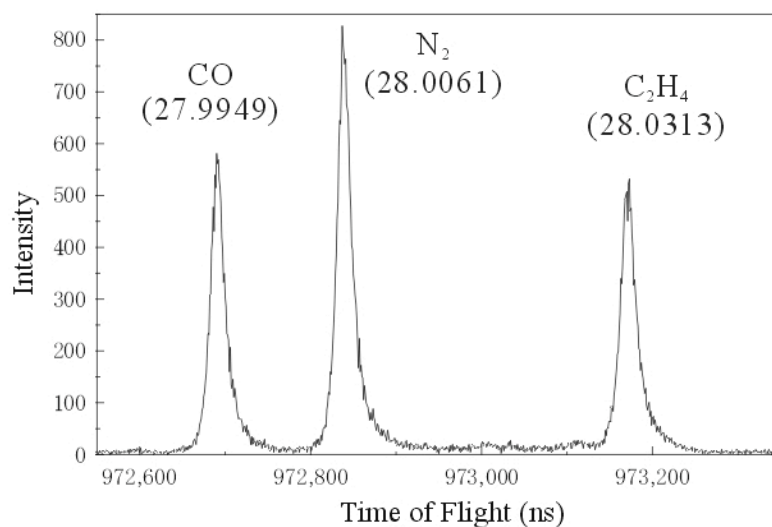


Fig. 22 Mass spectrum in an off-line test of the MR-TOF mass spectrometer. A mass resolving power of 60000 has been achieved in this measurement.

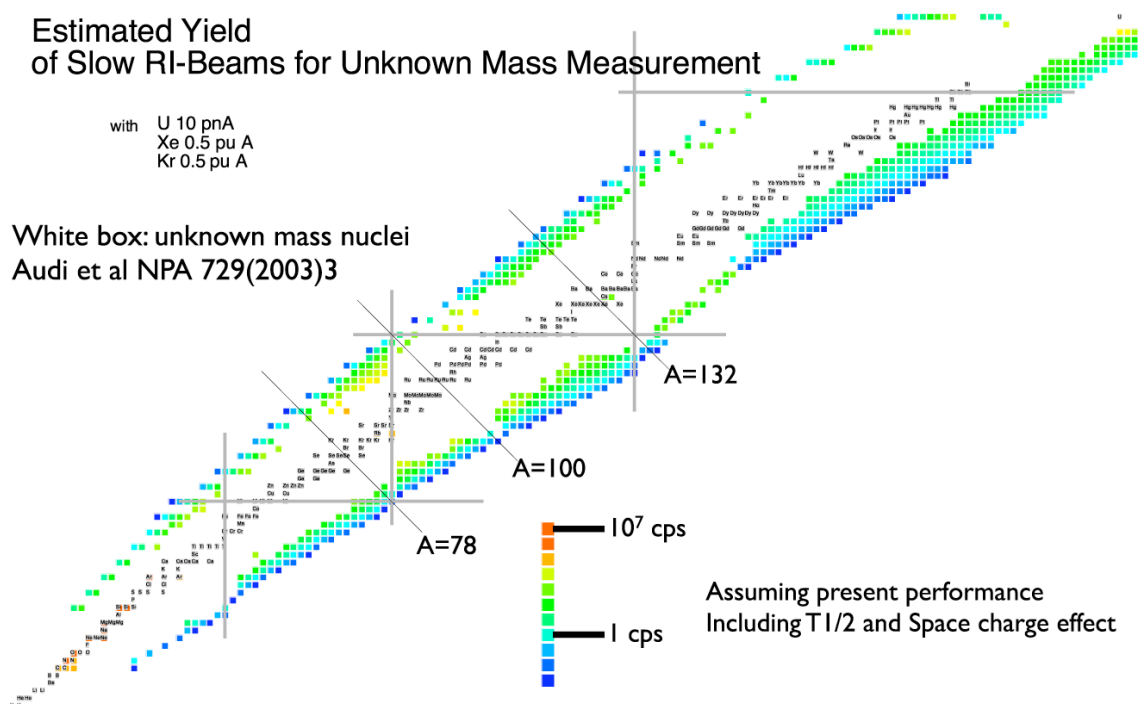


Fig. 23. Possible nuclides whose masses can be determined at SLOWRI. White boxes are the nuclides of which the mass has been determined already [15]. Note that recent measurements such as at ESR are not included in this figure.

2. Collinear laser spectroscopy

The root-mean-square charge radii of unstable nuclei have been determined exclusively by isotope shift measurements of the optical transitions of singly-charged ions or neutral atoms by laser spectroscopy. Many isotopes of alkaline, alkaline-earth, noble-gases and several other elements have been measured by collinear laser spectroscopy since these ions have all good optical transitions and are available at conventional ISOL facilities. However, isotopes of other elements especially refractory and short-lived ones have not been investigated so far.

In SLOWRI, isotopes of all atomic elements will be provided as well collimated mono-energetic beams. This should expand the range of applicable nuclides of laser spectroscopy. In the first years of the RIBF project, Ni and its neighboring elements, such as Ni, Co, Fe, Cr, Cu, Ga, Ge are planned to be investigated. They all have possible optical transitions in the ground states of neutral atoms with presently available laser systems (Fig. 25). Some of them have so called recycle transitions which enhance the detection probabilities noticeably. Also the multistep resonance ionization (RIS) method can be applied to the isotopes of Ni as well as those of some other elements. The required minimum intensity for this method can be as low as 10 atoms per second.

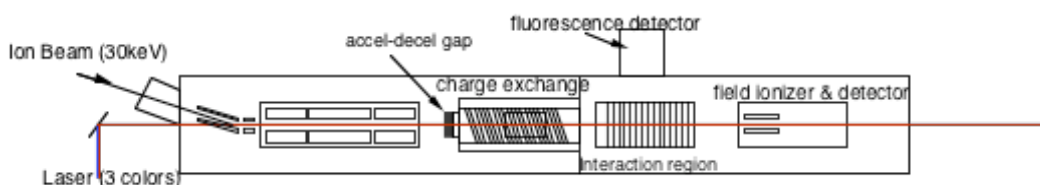


Fig. 24. Schematic of the collinear laser spectroscopy experimental setup.

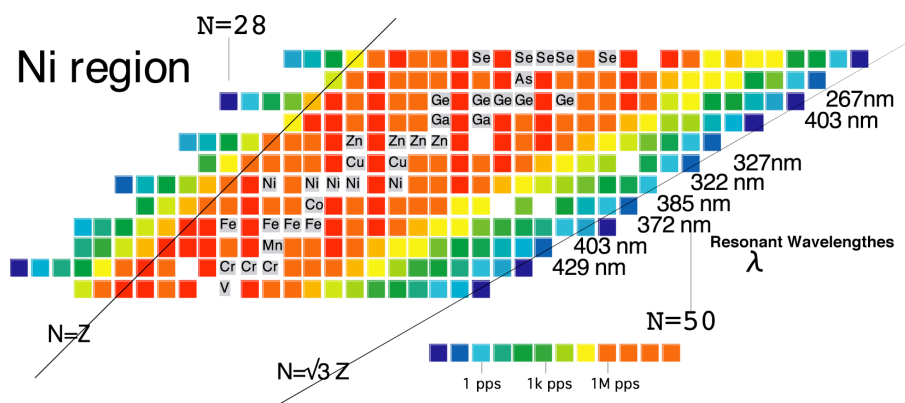


Fig. 25. Expected isotopes in the Ni region. Possible resonant wavelengths of the neutral atoms are also indicated also in the right side.

3. Hyperfine structure spectroscopy

The proton distributions in a nucleus can be studied by determining the charge radius of the nucleus, however, the neutron distributions are hard to be determined, since neutrons have no net electric charges but only have magnetization. High precision measurements of the ground state hyperfine splittings for a series of isotopes should enable us to study the isotope shift in the M1 term which is the so called differential hyperfine anomaly. The main part of this anomaly is due to the Bohr-Weisskopf effect which stems from the finite distribution of the magnetization in the inhomogeneous hyperfine field at the nucleus [16]. This effect would be particularly useful to investigate the root-mean-square radius of a valence neutron in case of neutron-odd nuclei.

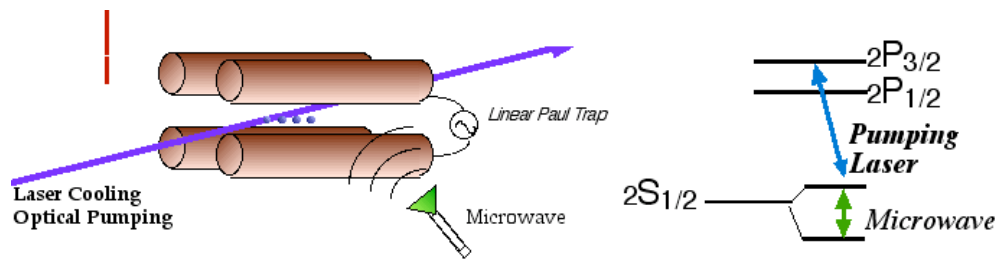


Fig. 26. Sketch of the linear Paul trap for HFS spectroscopy (left) and the pumping scheme of laser microwave double resonance spectroscopy (right).

For Be isotopes such experiments are already in progress at the present facility as phase-0 experiments of the SLOWRI project (Fig. 27) [17,18]. Be-11 is known as a neutron halo nucleus so that a large hyperfine anomaly is expected due to a large root-mean-square radius of the valence neutron of Be-11 [19]. The precision hyperfine structure spectroscopy would provide the first confirmation of halo nuclei with a reliable probe of electromagnetic interaction.

Other elements such as Mg, Ca, Sr, Ba and Ra are planned to be investigated at SLOWRI.

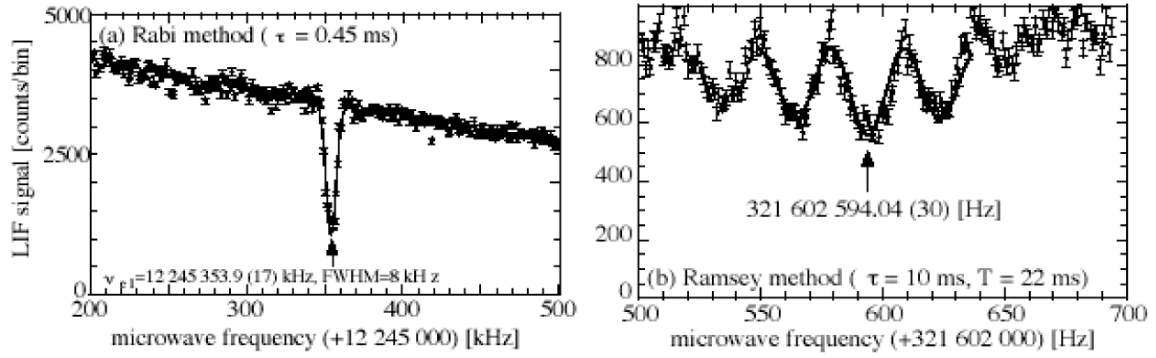


Fig. 27. Hyperfine structure spectroscopy spectra of Be-9 ions. From the electron spin flip transition frequency (left) and the nuclear spin flip transition frequency (right), the magnetic hyperfine constant A and the nuclear magnetic moment ratio g_I/g_J of Be-9 can be determined with accuracies of 10^{-9} and 10^{-7} , respectively.

VIII. UNIQUENESS

The combination of BigRIPS and the rf ion guide technique enables us to obtain universal slow RI-beams. The key technology of the planned facility is the rf ion guide which was developed by the present group at RIKEN [1]. Although there are several similar devices being build at other facilities worldwide [20, 21], only a few of them are in operation for high energy RI-beams. The SLOWRI facility will be a unique and single facility, at least, until RIA in the US or FAIR in Germany will operate.

Reference

- [1] M. Wada, Y.Ishida, T.Nakamura, Y.Yamazaki, T.Kambara, H.Ohyama, Y .Kanai, T.M.Kojima, Y.Nakai, N.Ohshima, A.Yoshida, T.Kubo, Y.Matsuo, Y.Fukuyama, K.Okada, T.Sonoda, S.Ohtani, K.Noda, H.Kawakami, I.Katayama, "Slow RI-beams from projectile fragment separators" Nucl. Instrum. and Meth. B204, 570-581 (2003)
- [2] H.J. Xu, M. Wada, J.Tanaka, H.Kawakami, I.Katayama, S.Ohtani, "A new cooling and focusing device for ion guide", Nucl. Instr. and Meth. A333, 274, (1993).
- [3] S. Masuda, K. Fujibayashi, K. Ishida, H. Inaba, "Confinement and transportation of charged aerosol clouds via electric curtain", IEEE, translation from Trans. IEE Japan, Vol. 92B (1972) 9-18.
- [4] A. Takamine, M. Wada, Y. Ishida, T. Nakamura, K. Okada, Y. Yamazaki, T. Kambara, Y. Kanai, T.M. Kojima, Y. Nakai, N. Oshima, A. Yoshida, T. Kubo, S. Ohtani, K. Noda, I. Katayama, P. Hostain, V. Varentsov, H. Wollnik, "Space-charge effect in the catcher gas cell of a rf ion guide" Rev. Sci. Instr. 76 1(2005) DOI: 10.1063/1.2090290
- [5] S. Fujitaka, M. Wada, H.Wang, J.Tanaka, H.Kawakami, I.Katayama, K.Ogino, H.Katsuragawa, T.Nakamura, K.Okada, S.Ohtani, "Accumulation of ions from a recoil mass separator in a new type of linear trap", Nucl. Instr. and Meth. B126, 386, (1997)
- [6] Nieminen, J. Huikari, A. Jokinen, J. Aysto, P. Campbell, ECA Cochrane, "Beam cooler for low energy radioactive ions", Nucl. Instr. Meth. A469 (2001) 244-253.
- [7] M.Wada, I.Katayama, H.Kawakami, J.Tanaka, S.Fujioka, Y.Ogino, H.Wang, K.Okada, T.Nakamura, S.Ohtani, "Nuclear laser spectroscopy with on-line traps", Hyperfine Interactions 103, 59, (1996).
- [8] N. Yamanaka, "Calculations of specific mass shifts in Be II (1s2 2s 2S, 1s2 2p 2p)", Phys. Lett. A243 (1998) 132
- [9] V. Varentsov and D. Habs, "'Fair-wind gas cell' – a new concept of a buffer gas cell design", Nucl. Instr. Meth. Phys. Res. A496, 286-292 (2003)
- [10] V. Varentsov and M. Wada, "Computer experiments on ion beam cooling and guiding in fair-wind gas cell and extraction RF-funnel system" Nucl. Instr. Meth. Phys. Res. A532, 210-215 (2004)
- [11] I. Katayama, M. Wada, H. Kawakami, J. Tanaka and K. Noda, "Cyclotron ion guide for energetic radioactive nuclear ions", Hyper. Inter. 115(1998)165 .
- [12] G. Bollen, D.J. Morrissey, S. Shwartz, "A study of gas-stopping of intense energetic rare isotope beams", Nucl. Instr. Meth. A550 (2005) 27-38.
- [13] T. Kubo, "In-flight RI beam separator BigRIPS at RIKEN and elsewhere in Japan", Nucl. Instr. Meth. B204 (2003) 97., and T. Suda, private communication.

- [14] Y. Ishida, M. Wada, Y. Matsuo, I. Tanihata, A. Casares, H. Wollnik, “A time-of-flight mass spectrometer to resolve isobars”
Nucl. Instr. and Method. B219-220, 468-472 (2004)
- [15] G. Audi, A.H. Wapstra, C. Thibault, “The AME2003 atomic mass evaluation”,
Nucl. Phys. A729 (2003)337-676
- [16] A. Bohr and V.F. Weisskopf, “The influence of nuclear structure on the hyperfine structure of heavy elements”,
Phys. Rev. 77 (1950) 94.
- [17] K. Okada, M. Wada, T. Nakamura, R. Iida, S. Ohtani, J. Tanaka, H. Kawakami and I. Katayama, "Laser-microwave double resonance spectroscopy of laser-cooled ${}^9\text{Be}^+$ ions in a weak magnetic field for studying unstable Be isotopes", J. Phys. Soc. Japan 67(1998)3073
- [18] T. Nakamura, M.Wada, K.Okada, I.Katayama, S.Ohtani, H.A.Schuessler, "Precision spectroscopy of the Zeeman splittings of the ${}^9\text{Be}^+ 2\ ^2\text{S}_{1/2}$ hyperfine structure for nuclear structure studies",
Opt. Comm. 205, 329-336 (2002)
- [19] T. Fujita, K. Ito, T. Suzuki, “Hyperfine anomaly of Be isotopes and anomalous large anomaly in ${}^{11}\text{Be}$ ”,
Phys. Rev C59 (1999) 210.
- [20] G. Savard, J. Clark, C. Boudreau, F. Buchinger, J.E. Crawford, H. Geissel, J.P. Greene, S. Gulick, A. Heinz, J.K.P. Lee, A. Levand, M. Maier, G. Munzenberg, C. Scheidenberger, D. Seweryniak, K.S. Sharma, G. Sprouse, J. Vaz, J.C. Wang, B.J. Zabransky, Z. Zhou, the S258 Collaboration, “Development and operation of gas catchers to thermalize fusion-evaporation and fragmentation products”,
Nucl. Instr. Meth. B204 (2003) 582-586.
- [21] S. Schwartz, G. Bollen, D. Lawson, P. Lofy, D.J. Morrissey, J. Ottarson, R. Ringle, P. Schury, T. Sun, V. Varentsov, L. Weissman, “The low-energy-beam and ion-trap facility at NSCL/MSU”,
Nucl. Instr. Meth. B204 (2003) 507-511